Journal of Materials Research and Technology 38 (2025) 3243–3250

Contents lists available at ScienceDirect

Journal of Materials Research and Technology

journal homepage: www.elsevier.com/locate/jmrt

An innovative route for incorporating pharmaceuticals into biodegradable metal matrices for drug delivery implants

Debora R. Lopes [a], Amanda P. Carvalho [a], Maiara C. de Miranda [b], William Gustavo Lima [b], Talita Martins [a], Augusta Isaac [a], Rachel B. Caligiorne [b], Livia Cupertino-Malheiros [c], Megumi Kawasaki [d], Eduardo Henrique M. Nunes [a], Roberto B. Figueiredo [a,*]

[a] Department of Metallurgical and Materials Engineering, Universidade Federal de Minas Gerais, Belo Horizonte, MG, 31270-901, Brazil
[b] Programa de Pós-Graduação Stricto Sensu em Medicina e Biomedicina, Faculdade de Saúde Santa Casa de BH, Belo Horizonte, Minas Gerais, Brazil
[c] Department of Civil & Environmental Engineering, Imperial College London, London, SW7 2AZ, UK
[d] School of Mechanical, Industrial and Manufacturing Engineering, Oregon State University, Corvallis, OR, 97331, USA

ARTICLE INFO

Handling editor: M Meyers

Keywords:
Drug delivery
Biodegradable metal
Metal matrix composite
High pressure torsion

ABSTRACT

Metal particles can be welded without significant heating due to severe plastic deformation caused by high pressure torsion. This process has been used to consolidate metallic particles and incorporate ceramic materials into a metallic matrix. The present study demonstrates for the first time that this technique can also be used to incorporate pharmaceuticals into a metallic matrix. In addition, it shows that embedding pharmaceuticals in a biodegradable metal matrix enables the creation of composites with drug delivery capabilities. The results obtained here indicate the successful incorporation of ofloxacin, amphotericin B, and diclofenac sodium into a continuous magnesium matrix. The antifungal and antibacterial activities of the different composites are evaluated along with their drug release kinetics. A new class of biomaterials, biodegradable metals with integrated drug delivery functionality, is introduced in this study.

1. Introduction

Biodegradable metals have attracted much attention for their ability to create temporary structural implants. These implants could play a structural role, such as in stents [1] and orthopedic applications [2], allowing tissue regeneration while the material undergoes continuous corrosion. The by-products must be non-toxic and should be absorbed and eliminated by the body. Metallic materials are good candidates because of their high strength and toughness. Some metals, such as titanium and stainless steel, form stable oxide coatings on their surfaces that prevent continuous corrosion and make them suitable for permanent implantation. In contrast, metals such as magnesium, iron, and zinc form less stable oxide layers in physiological environments, which can lead to ongoing corrosion [3].

To improve the performance of biodegradable metals, extensive efforts have been made to understand the influence of alloying elements [4,5] and structural features [6–9] on their mechanical properties and corrosion behavior. Additionally, there is growing interest in the development of hybrid materials. For instance, bioactive particles can be incorporated into biodegradable metal matrices [10–13], or bioactive material coatings can be deposited on the metal surface [14–17], improving their functionality and performance in biomedical applications.

High-Pressure Torsion (HPT) has proven to be a powerful processing technique for improving the performance of biodegradable metals. For example, this technique produces grain refinement that can improve the strength and reduce the corrosion rate of magnesium and its alloys [18–20]. In addition, it has been known for nearly 90 years that metallic materials can “self-weld” under compressive and torsional shear stresses [21]. Therefore, HPT has been used not only to blend biodegradable metals such as Mg/Fe [22] and Mg/Zn [23–25], but also to consolidate biodegradable metals with bioactive particles to form hybrid materials [26–28]. This processing technique has also been used to consolidate inert metal particles with proteins [29].

The incorporation of different materials dispersed into a metallic matrix is usually achieved by melting the metal or by high temperature extrusion. A key advantage of HPT processing is its ability to consolidate metallic particles without the need for heating, which allows for the

* Corresponding author.
E-mail address: figueiredo@demet.ufmg.br (R.B. Figueiredo).

https://doi.org/10.1016/j.jmrt.2025.08.095
Received 2 July 2025; Received in revised form 8 August 2025; Accepted 13 August 2025
Available online 13 August 2025

inclusion of temperature-sensitive materials. This capability could make the incorporation of temperature-sensitive pharmaceuticals into a biodegradable metal matrix possible, leading to implants with drug delivery capabilities. The drug delivery capabilities of magnetic polymers [30,31] and metals nanoparticles [32] are well documented. This study aims to evaluate the potential of HPT for consolidating magnesium matrix composites with various pharmaceuticals, including antibiotics, antifungals, and anti-inflammatories. Implants loaded with active pharmaceutical ingredients provide precise drug delivery to the target site while maintaining optimal drug concentrations. This approach increases drug delivery efficiency, reduces dosing frequency, and improves patient compliance, ultimately leading to significantly better clinical outcomes. In addition, controlled and localized drug release plays a critical role in minimizing side effects that could otherwise compromise implant integration and lead to failure [33,34].

2. Experimental procedure

The materials used in this study were commercial grade magnesium particles, commercial grade magnesium, magnesium alloy ZK60, pharmaceuticals, and BSA (Bovine serum albumin). The pharmaceuticals used were ofloxacin (antibacterial), amphotericin B (antifungal), and diclofenac sodium (anti-inflammatory). The samples were prepared by mixing the metallic particles with different drugs or BSA protein. The process is shown schematically in Fig. 1. The raw materials were first hand-mixed in pre-determined proportions and then pressed at approximately 400 MPa to produce 8 mm diameter, 1.2 mm thick discs (precompacts). Heterogeneity in phase distribution was not visibly observed in any of the precompacts. Sixteen discs were processed by HPT at room temperature using a quasi-constrained setup, operating at a nominal pressure of 4 GPa and a rotational speed of 1 rpm. The processed discs had 8 mm diameter and 0.7 mm thickness. The first batch of samples was produced mixing pure magnesium particles with 5 wt% diclofenac sodium, 5 wt% ofloxacin and 5 wt% BSA. The amount of pharmaceuticals was reduced in other samples, including the samples

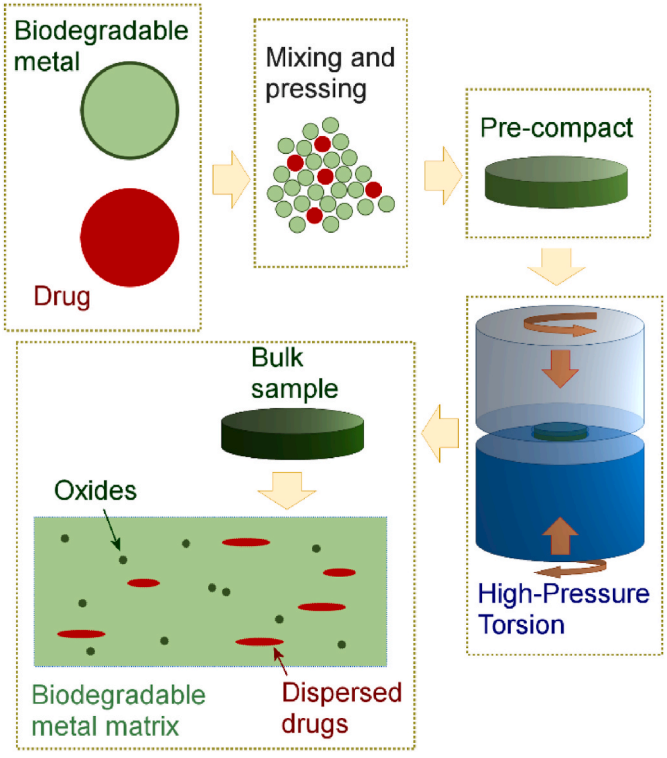

Fig. 1. Illustration of the process used to mix and consolidate biodegradable particles with drugs.

with amphotericin, in order to improve consolidation and dispersion. Also, the magnesium alloy ZK60 was used in place of pure magnesium in selected samples in order to reduce the corrosion rate of the composite. The processed discs were then characterized for structural and mechanical properties and evaluated for drug release behavior.

Samples examined by scanning electron microscopy (SEM) and energy dispersive spectroscopy (EDS) were ground and polished using standard metallographic procedures prior to analysis. Electron-transparent, nanometer-thick lamellae were also extracted from the disc of a Mg-5 % ofloxacin composite using a focused ion beam (FIB) milling apparatus and analyzed by transmission electron microscopy (TEM). The amphotericin and ofloxacin pure pharmaceuticals and disks of Mg-5 % ofloxacin and Mg-2.5 % amphotericin were characterized using Fourier transform infrared spectroscopy (FTIR). These tests were performed on a Bruker Alpha spectrometer using an attenuated total reflectance (ATR) mode and a diamond crystal as the reflecting element. Spectra were collected with a resolution of 4 cm^{-1} and 128 scans. Plane strain compression tests [35] were used to evaluate the stress-strain relationship in selected samples.

Kirby-Bauer assay was used to evaluate the antimicrobial activity of selected composites, in accordance with the Clinical and Laboratory Institute (CLSI) [36]. All the microorganisms employed were originated from the American Type Culture Collection (ATCC™) and provided by the Microbiology Reference Laboratory of the Oswaldo Cruz Foundation (FIOCRUZ™; Rio de Janeiro, RJ, Brazil). The antifungal activity was determined against *Candida albicans* ATCC 10231, using discs functionalized with amphotericin B, and the antibacterial effect was determined against *Staphylococcus aureus* ATCC 29213 to the discs functionalized with ofloxacin. According to ATCC™ specifications, *C. albicans* 10231 is resistant to anidulafungin, voriconazole, itraconazole and fluconazole.

To evaluate the activity of disks containing ofloxacin (Sigma-Aldrich™; St. Louis, USA), Mueller-Hinton agar plates (Kasvi™; São José dos Pinhais, Brazil) were initially inoculated over their entire surface with swabs soaked in an inoculum of *S. aureus* at 10^8 CFU/mL prepared in sterile saline (0.85 % NaCl; Synth™; Diadema Brazil). After inoculation, the plates were dried in an incubator at 37 °C for 15 min and then circles of 8 mm in diameter were cut from the surface of the medium. The wells formed were filled with 100 μL of sterile saline (0.85 % NaCl) and the disks were added inside. Next, the plates were incubated for 24 h at 37 °C and the inhibition zone was determined with the aid of a millimeter ruler. Discs without the antimicrobial were included as a negative control and the experiment was carried out in triplicate [36]. The discs functionalized with amphotericin B (Sigma-Aldrich™; St. Louis, USA) were tested against *C. albicans*. An inoculum containing 10^6 CFU/mL of this yeast used to seed the surface of Sabouraud-dextrose agar (Kasvi™; São José dos Pinhais, Brazil). After drying for 15 min at 37 °C in an incubator, wells were cut on the surface of the agar, filled with saline (NaCl 0.85 %), and the discs were inserted. After incubation at 37 °C for 48 h, the inhibition zones were measured. The experiment was performed in triplicate and discs without antifungal agent were used as negative control [37].Finally, the inhibition zones between the antimicrobial-containing discs and the control discs were compared using the Student's *t*-test in GraphPad Prism™ version 8, being considered p-value less than 0.05 to a significantly difference.

To evaluate the drug release behavior of the prepared materials, discs of Mg-diclofenac sodium and magnesium alloy ZK60-diclofenac sodium were immersed in Hank's solution (Sigma Aldrich H4891) with 0.35 gL^{-1} sodium bicarbonate to stabilize the pH. During various time intervals, the solution was collected. These aliquots were transferred to quartz cuvettes and analyzed using a Shimadzu UV-2600 spectrometer with a resolution of 1 cm^{-1}, and the absorbance at 276 nm was used as the reference for diclofenac sodium. The drug concentration in the aliquots was determined using a previously obtained calibration curve with an R^2 value of 0.999, according to the Beer-Lambert law.

A disc of Mg-2 % diclofenac sodium composite was analyzed using X-ray tomography (XRT) after 24 h of immersion in Hank's solution. Imaging was performed with a ZEISS Xradia 610 Versa 3D X-ray microscope (Carl Zeiss AG, Germany) to evaluate the disc's integrity and visualize the three-dimensional spatial distribution of different phases, including corrosion products and the matrix. The X-ray tube voltage and current were set to 60 kV and 110 μA, respectively. Each tomographic scan consisted of approximately 2000 radiographs acquired over a full 360° rotation, with an exposure time of 4 s per image, totaling 2 h 22 min of scanning. The relative positioning of the X-ray source, sample, and detector, combined with a 0.4 × objective, resulted in a pixel size of 3.33 μm. Image analysis and visualization were performed using Avizo Software (Thermo Fisher Scientific Inc., USA).

3. Results

3.1. Consolidation

The consolidation of the metallic particles and incorporation of the pharmaceuticals were evaluated by microstructural observation and conventional mechanical testing. Fig. 2 shows SEM images of Mg-diclofenac sodium, Mg-ofloxacin and Mg-BSA composites processed after 10 turns of HPT (N = 10). The low magnification images at the top of Fig. 2 reveal the successful consolidation of the particles and the formation of a continuous metallic matrix with dispersed phases. However, the morphology of the phases varies. The BSA-containing composite is characterized by long, thin phases. Higher magnification images and EDS mapping show that these thin dark phases are rich in carbon and oxygen, confirming the presence of BSA. This morphology is not ideal, as the long continuous interface between the magnesium matrix and the protein can serve as preferential pathways for crack and corrosion propagation. Better phase dispersion was achieved in the Mg-based composites. A continuous magnesium matrix with discontinuous dispersion of other phases is observed in these cases. A higher-magnification SEM image and EDS mapping of the Mg-diclofenac sodium composite, shown in Fig. 2, reveal that the dark phase is devoid of magnesium and is instead enriched in carbon and sodium, consistent with the chemical composition of diclofenac sodium.

The grain structure in the metallic matrix and the interface between the metallic matrix and the pharmaceutical phase were characterized using TEM. An electron-transparent lamella was extracted from the interface between the phases in the Mg-5 % ofloxacin composite using FIB. Fig. 3 presents representative images of the interface between magnesium and ofloxacin, along with the selected area electron diffraction (SAED) pattern and compositional mapping. A polycrystalline structure with an average grain size of about 200 nm is observed in the metallic matrix. Such a small grain size confirms that the severe plastic deformation route effectively refines the grain structure of the metallic material in addition to consolidating the particles. No crystal structure was identified in the pharmaceutical phase and the SAED pattern confirms that this phase is amorphous. The composition maps show a clear separation between the metallic matrix and the pharmaceutical phase. This suggests that there was no mixing or reaction between the different materials.

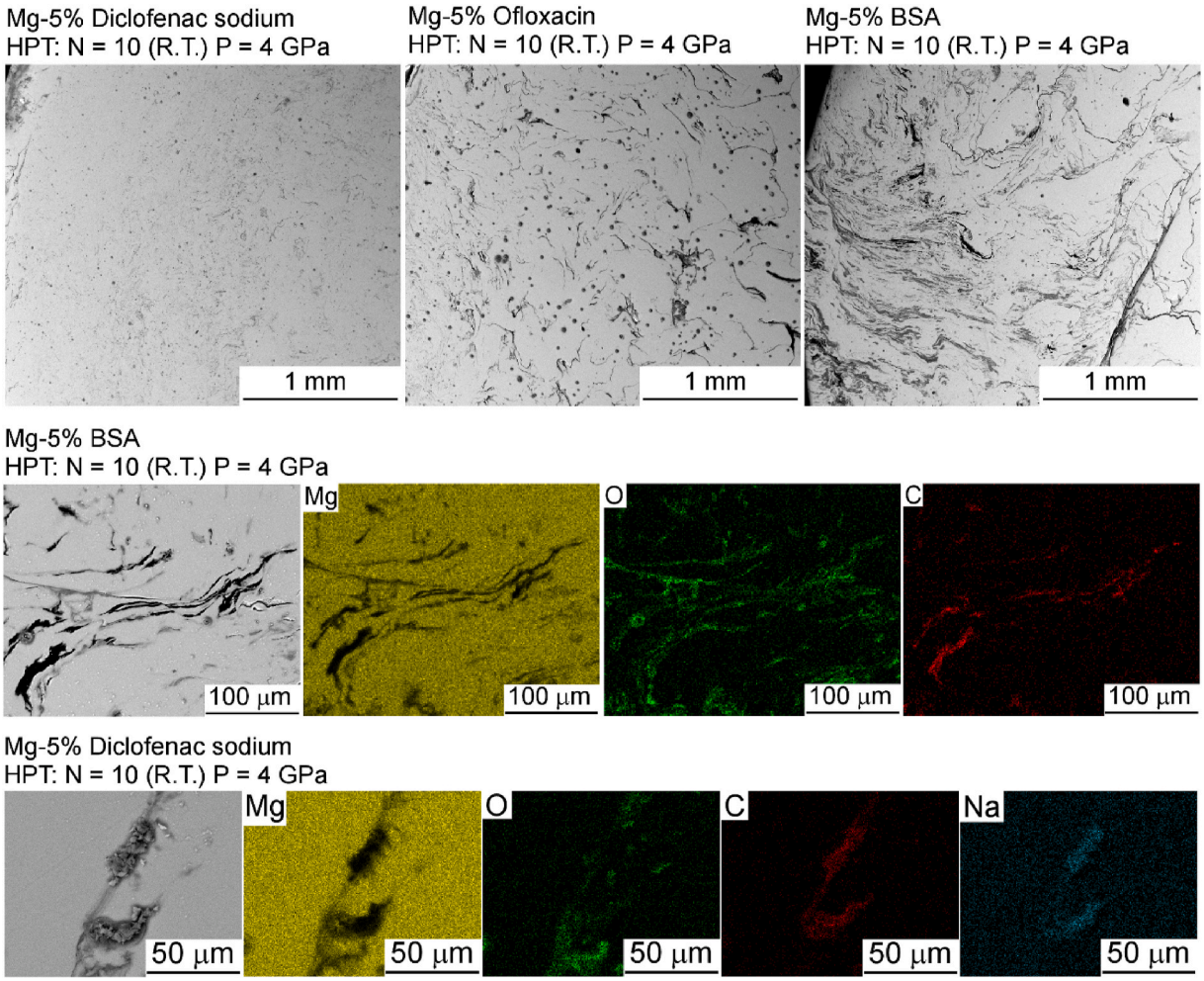

Fig. 2. Scanning electron microscopy images of Mg-diclofenac sodium, Mg-ofloxacin and Mg-bovine serum albumin (BSA) composites.

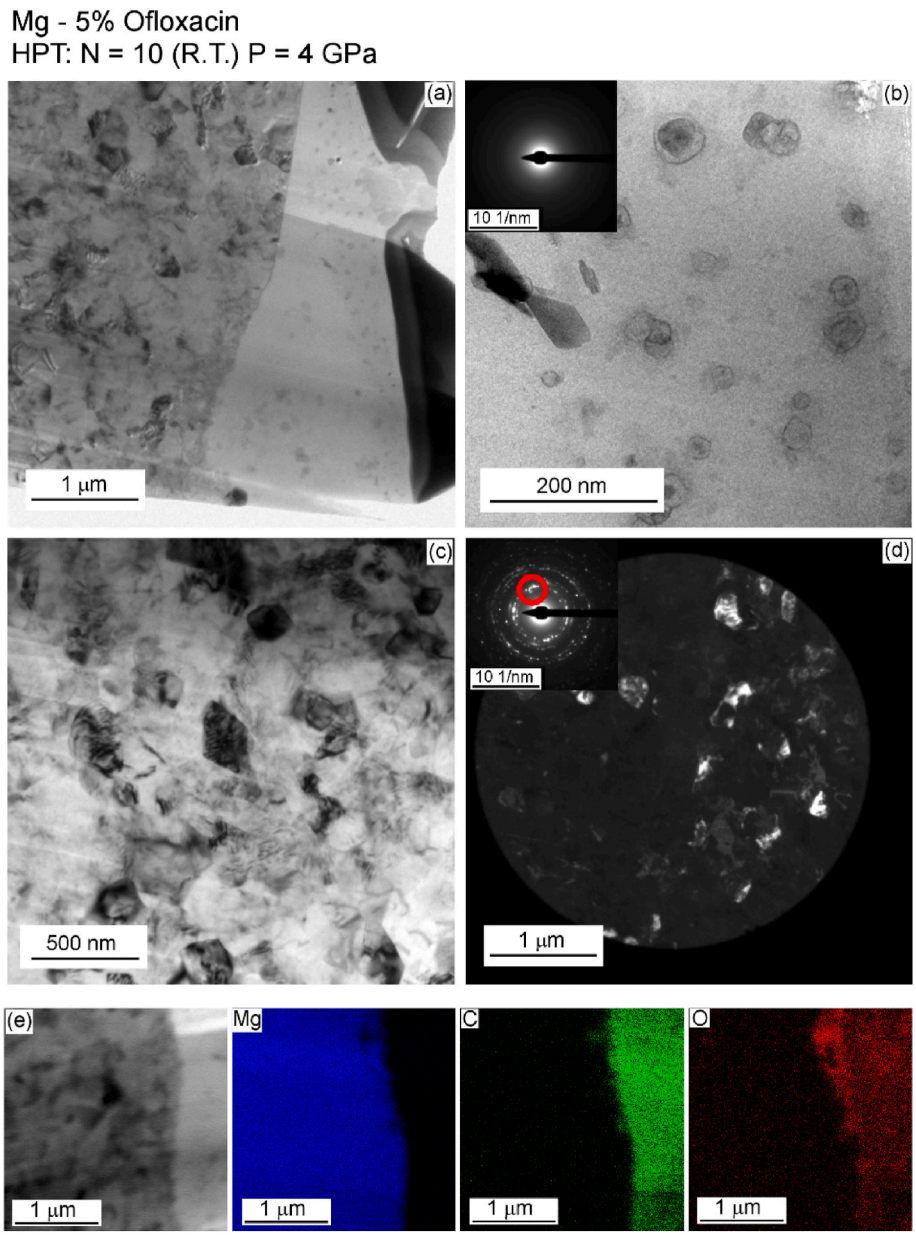

Fig. 3. Transmission electron microscopy images of the interface between the metallic matrix and the pharmaceutical phase in the Mg-5 % ofloxacin composite.

The consolidation was further assessed by mechanical testing through plane strain compression. Fig. 4 shows the stress-strain curves obtained by testing pure magnesium, Mg-BSA, and Mg-diclofenac sodium composites consolidated by high pressure torsion. The results are compared to bulk pure magnesium processed by HPT [35]. Samples consolidated from particles show increased strength compared to bulk magnesium, confirming good consolidation. The strength of the Mg-BSA composite is slightly lower than that of Mg-diclofenac sodium, suggesting that the long and thin dispersion of the protein may compromise the strength due to the increased interface between the different phases. In contrast, the higher strength observed in the particle consolidated samples is attributed to the presence of second phases, including magnesium oxide, dispersed in the matrix, which promotes grain refinement.

3.2. Antimicrobial activity

The presence of the pharmaceuticals and the ability of the composite to degrade and release them were assessed. Thus, FTIR was used to evaluate the presence of antibacterial and antifungal pharmaceuticals in samples of Mg-5 % ofloxacin and Mg-2.5 % amphotericin B composites. Fig. 5a shows the absorbance spectrum of pure pharmaceuticals and the composites containing them. Both amphotericin B and ofloxacin exhibit absorption bands in the spectral region below 1600 cm^{-1}, and the composites show enhanced absorption in this region. However, the bands are less well defined in the composites due to the reduced volume of drugs present in them. The release of these drugs was evaluated by immersing the composites in media containing either fungi or bacteria. Thus, Fig. 5b shows images of the samples placed in plates containing *S. aureus* and *C. albicans* after 24 and 48 h of incubation, respectively. The Mg-2.5 % amphotericin B produced an inhibition halo of 23 ± 2 mm against *C. albicans*, which was significantly greater than that observed with discs not impregnated with antifungal agent (8 ± 0.6 mm; p-value <0.0001). The Mg-5 % ofloxacin, in turn, exhibits an inhibition halo of 50 ± 6 mm against *S. aureus*, which is significantly larger than that observed in control discs (6 ± 0,2 mm; p-value <0.0001).

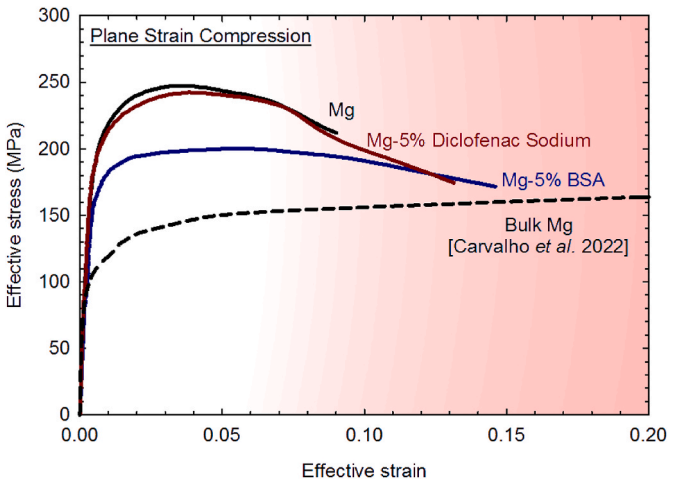

Fig. 4. Stress vs. Strain curves obtained by plane strain compression tests in pure Mg and Mg-BSA and Mg-diclofenac Sodium composites consolidated by HPT. Data from the literature [35] for bulk magnesium is also shown for comparison.

3.3. Release of pharmaceutical

Initial attempts to evaluate drug release in Mg-diclofenac sodium composites indicated rapid corrosion of the samples. The Mg-5 % diclofenac sodium samples fragmented into multiple pieces after 24 h of immersion in Hank's solution. As a result, samples with lower drug levels were prepared and showed improved corrosion resistance. Although the discs did not fracture, they show signs of significant corrosion. X-ray microtomography was used to evaluate the integrity of an Mg-2 % diclofenac sodium composite disc after 24 h of immersion in Hank's solution. Fig. 6a and b shows representative plane-view and cross-sectional images of the disc, respectively. The image contrast refers to the varying X-ray attenuation values of the different phases present in the disc. Continuous areas of lower attenuation (darker areas) and higher attenuation (brighter areas) are clearly distinguished throughout the plane view of the disc, corresponding to corrosion products and bulk metal, respectively. The images were then segmented into these two distinct phases based on a user-defined gray level threshold. Fig. 6c shows 3D images of the disc, with the bulk metal rendered in blue and the corrosion product in yellow. Corrosion products were observed not only on the surface of the discs but also within the interior. These products propagated along continuous surfaces, indicating a loss of integrity after 24 h of immersion. The corrosion product layers tended to align parallel to the disc surface, corresponding to the shear plane during HPT processing.

The analysis of the corrosion behavior of the Mg-diclofenac sodium composite suggested that corrosion propagates along the shear plane of HPT processing and this behavior is attributed to the alignment of the pharmaceutical phase to the shear plane during consolidation. In order to avoid the formation of such alignment a different procedure was adopted to produce the composites. A hole was made near the edges of discs of bulk magnesium, a mixture of magnesium particles with the pharmaceutical was introduced into this role and the sample was thus consolidated using high pressure torsion. This procedure granted significant improvement in corrosion resistance of the composite. Also, a sample of magnesium alloy ZK60 (Mg-5.5 % Zn-0.5 % Zr) was used instead of pure magnesium.

The ZK60-2 % diclofenac sodium composite exhibits good corrosion resistance even after 3 weeks of immersion in Hank's solution. Fig. 7 shows the cross-section of the specimen, where a continuous metallic matrix is observed across most of the disc. Significant corrosion was confined to the edge portions, where the drug was introduced. Despite this localized corrosion, the disc maintained its overall integrity.

Drug release was evaluated by immersing the discs in Hank's solution. The amount of the pharmaceutical in the solution is plotted as a function of immersion time in Fig. 8. A rapid release is observed in the Mg-2 % diclofenac sodium prepared from the consolidation of particles showing rapid corrosion, while a gradual release is observed in the ZK60-2 % diclofenac sodium composite prepared using the hole in a bulk disc procedure. This confirms that the latter display controlled corrosion and release ability.

4. Discussion

Experiments have shown that HPT allows the mixing of different metals [23–25,38,39] while also favoring the incorporation of ceramic phases [40], bioactive materials [26–28] and protein [29]. Welding at room temperature is achieved by severe shearing of the metallic

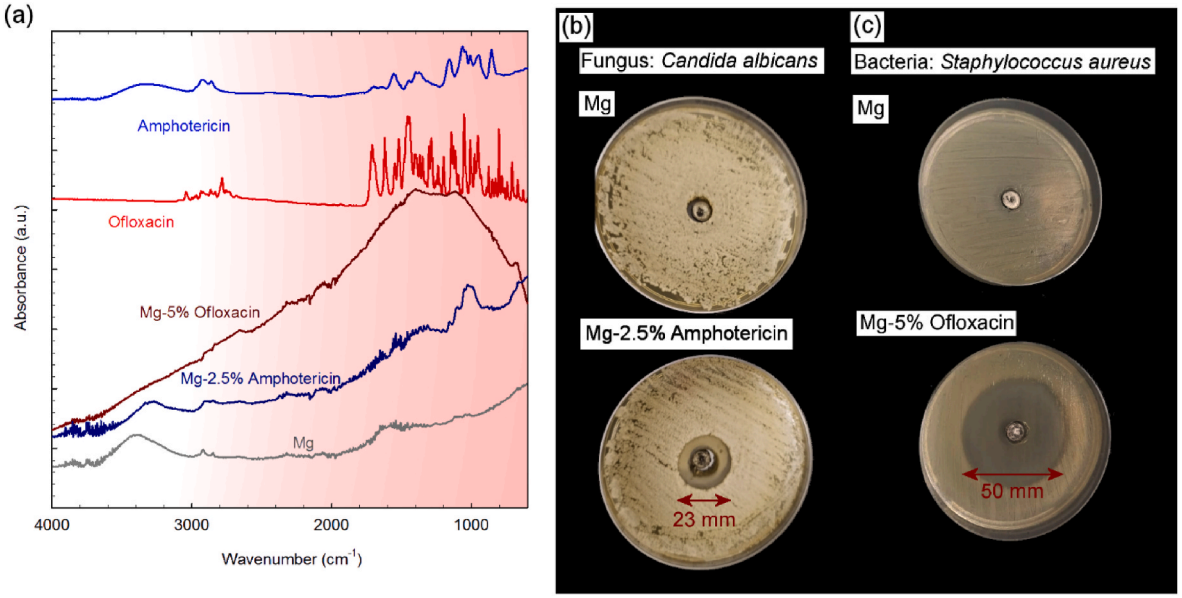

Fig. 5. (a) FTIR absorbance curves of pure Mg and pure pharmaceuticals and the composites containing both and (b) photos of plates containing fungus and bacteria after 24 h immersion of pure magnesium and Mg-pharmaceuticals composites.

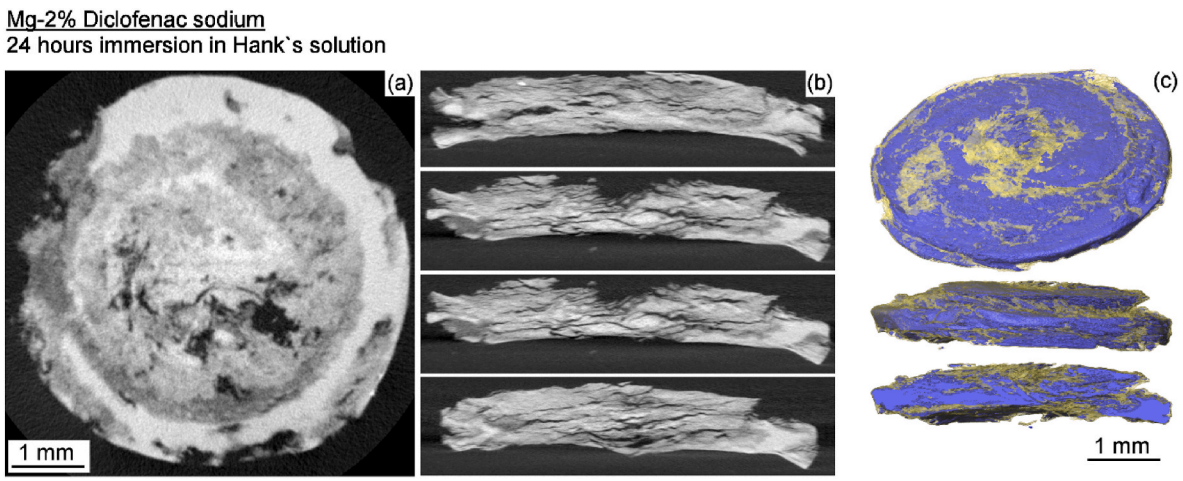

Fig. 6. X-ray tomography images of Mg-2 % diclofenac sodium composite after 24 h of immersion in Hank's solution. Representative plane-view image (a) and cross-sectional images (b) of the disc. Three-dimensional images of the disc, with the bulk metal rendered in blue and the corrosion product in yellow (c).

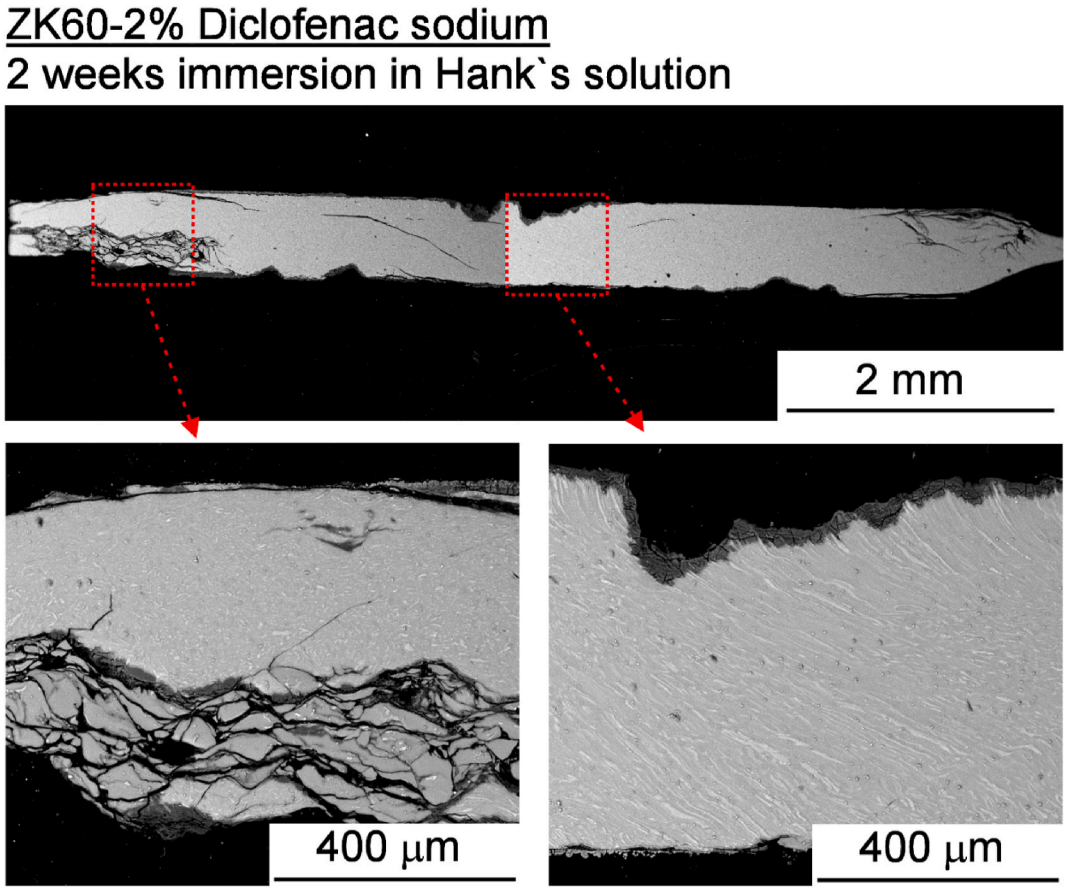

Fig. 7. Cross section images of a disc of ZK60-2 % diclofenac sodium composite after 2 weeks of immersion in Hank's solution.

particles, which breaks the oxide layer and promotes metallic bonding. This study shows that the same principle applies when drugs are mixed with metallic particles. If the drugs can withstand the high pressure and shear, they become embedded in the bulk metal matrix. Analysis of the phase morphology shows that the drugs tend to align with the shear plane. It is expected that the bonding between the pharmaceuticals and the metallic phase is not as strong as the bonding within the metallic phase. Therefore, the drug-metal interface may have a lower shear resistance, and therefore there will be preferential sliding between the metal and the drug, resulting in phase alignment. Such alignment can be detrimental to corrosion resistance, as demonstrated by the lack of integrity of the Mg-diclofenac sodium composite immersed in Hank's solution for 1 day. This situation poses a challenge for the design of processing routes capable of avoiding the formation of continuous drug layers within the metallic matrix. In the present study, a solution is presented in which the drugs are mixed with metallic particles and incorporated into a hole of a bulk disk. In addition, further experiments should be carried out using biodegradable materials with higher

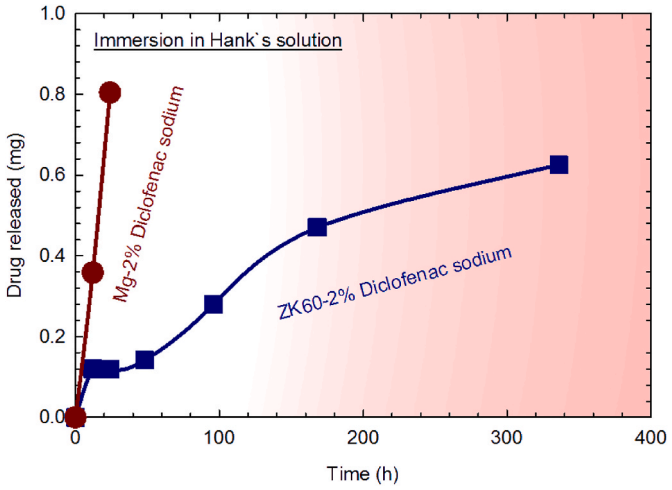

Fig. 8. Amount of diclofenac sodium released in Hank's solution as a function of immersion time.

corrosion resistance than magnesium. Zinc and iron may be suitable candidates, and recent experiments have shown that it is possible to incorporate hydroxyapatite and bioactive glass particles into a zinc matrix using HPT processing [26].

It is worth noting that solid state reaction has been reported during high pressure torsion processing. Mechanical mixing might take place between metals [41–43] and redox reaction has been reported between Nb_2O_5 with aluminum [44] and with magnesium [45]. Provided the number of rotations is large enough, typically in the range of hundreds, complete mixing in the atomic level can develop between different metallic materials [46,47]. Therefore, the number of rotations in the present experiments was limited to a maximum of 10 to avoid any reaction between the metallic phase and the drugs. Observation of the interface between the phases (Fig. 3) suggested that such reactions did not take place. In addition, the pharmaceutical activity was still retained, as shown by good antifungal and antimicrobial activity of the Mg amphotericin B and Mg ofloxacin composites.

5. Summary and conclusions

In this work, different drugs (ofloxacin, amphotericin B, and diclofenac sodium) and bovine serum albumin were mixed with particles of a biodegradable metal (magnesium) and consolidated at room temperature using high-pressure torsion. The resulting biodegradable metal-drug composites exhibited a continuous metal matrix with a discontinuous dispersion of the incorporated drugs. The severe plastic deformation process refined the grain structure of the metal matrix, and the composites exhibited high mechanical strength. Effective drug release was confirmed by the formation of inhibition halos in bacterial and fungal culture plates for composites containing the antibiotic and antifungal agents, respectively. In contrast, no such antimicrobial activity was observed in pure magnesium. The rapid corrosion of the Mg-diclofenac sodium composite led to a fast release of diclofenac sodium. However, modifying the processing route and replacing pure magnesium with the magnesium alloy ZK60 significantly improved corrosion resistance, enabling a more controlled release of diclofenac sodium over two weeks of immersion in Hank's solution.

CRediT authorship contribution statement

Debora R. Lopes: Investigation, Methodology, Writing – review & editing. **Amanda P. Carvalho:** Investigation, Writing – review & editing. **Maiara C. de Miranda:** Investigation, Methodology, Writing – review & editing. **William Gustavo Lima:** Investigation, Methodology, Writing – review & editing. **Talita Martins:** Methodology, Writing – review & editing. **Augusta Isaac:** Investigation, Methodology, Writing – review & editing. **Rachel B. Caligiorne:** Resources, Methodology, Writing – review & editing. **Livia Cupertino-Malheiros:** Project administration, Writing – review & editing. **Megumi Kawasaki:** Project administration, Writing – review & editing. **Eduardo Henrique M. Nunes:** Resources, Methodology, Project administration, Writing – review & editing. **Roberto B. Figueiredo:** Conceptualization, Funding acquisition, Resources, Methodology, Project administration, Writing – review & editing.

Declaration of competing interest

The authors declare that they have no known competing financial interests or personal relationships that could have appeared to influence the work reported in this paper.

Acknowledgements

The authors acknowledge financial support from CNPq, CAPES and FAPEMIG.

References

[1] Zong J, He Q, Liu Y, Qiu M, Wu J, Hu B. Advances in the development of biodegradable coronary stents: a translational perspective. Mater Today Bio 2022;16:100368.
[2] Chandra G, Pandey A. Biodegradable bone implants in orthopedic applications: a review. Biocybern Biomed Eng 2020;40:596–610.
[3] Zheng YF, Gu XN, Witte F. Biodegradable metals. Mater Sci Eng R Rep 2014;77:1–34.
[4] Shi Z-Z, Gao X-X, Zhang H-J, Liu X-F, Li H-Y, Zhou C, et al. Design biodegradable Zn alloys: second phases and their significant influences on alloy properties. Bioact Mater 2020;5:210–8.
[5] Li H, Wang P, Lin G, Huang J. The role of rare Earth elements in biodegradable metals: a review. Acta Biomater 2021;129:33–42.
[6] Zberg B, Ugowitzer PJ, Loffler JF. MgZnCa glasses without clinically observable hydrogen evolution for biodegradable implants. Nat Mater 2009;8:887–91.
[7] Parfenov EV, Kulyasova OB, Mukaeva VR, Mingo B, Farrakhov RG, Cherneikina YV, et al. Influence of ultra-fine grain structure on corrosion behaviour of biodegradable Mg-1Ca alloy. Corros Sci 2020;163:108303.
[8] Ge Q, Dellasega D, Demir AG, Vedani M. The processing of ultrafine-grained Mg tubes for biodegradables stents. Acta Biomater 2013;9:8604–10.
[9] Batista BA, Soares RB, Lins VFC, Figueiredo RB, Hohenwarter A, Matencio T. Corrosion in Hank's solution and mechanical strength of ultrafine-grained pure iron. Adv Eng Mater 2020;22:2000183.
[10] Zhang Z, Liu D, Chen Z, He X, Li X, Sun X. Fabrication, in vitro and in vivo properties of β-TCP/Zn composites. J Alloys Compd 2022;913:165223.
[11] Yang H, Qu X, Lin W, Wang C, Zhu D, Dai K, et al. In vitro and in vivo studies on zinc-hydroxyapatite composites as novel biodegradable metal matrix composite for orthopedic applications. Acta Biomater 2018;71:200–14.
[12] Witte F, Feyerabend F, Maier P, Fischer J, Störmer M, Blawert C, et al. Biodegradable magnesium–hydroxyapatite metal matrix composites. Biomaterials 2007;28:2163–74.
[13] Ratna Sunil B, Ganapathy C, Sampath Kumar TS, Chakkingal U. Processing and mechanical behavior of lamellar structured degradable magnesium–hydroxyapatite implants. J Mech Behav Biomed Mater 2014;40:178–89.
[14] Singh N, Batra U, Kumar K, Ahuja N, Mahapatro A. Progress in bioactive surface coatings on biodegradable Mg alloys: a critical review towards clinical translation. Bioact Mater 2023;19:717–57.
[15] Braga JdO, dos Santos DMM, Cotting F, Lins VFC, Leão NM, Soares DCF, et al. Surface modification of magnesium with a novel composite coating for application in bone tissue engineering. Surf Coating Technol 2022;433:128078.
[16] Braga JdO, de Carvalho SM, Silva LMC, Soares RB, Lins VFC, Mazzer EM, et al. Fabrication and characterization of dicalcium phosphate coatings deposited on magnesium substrates by a chemical conversion route. Surf Coating Technol 2020;386:125505.
[17] Vishwakarma V, Kaliaraj GS, Amirtharaj Mosas KK. Multifunctional coatings on implant materials—A systematic review of the current scenario. Coatings 2023;13:69.
[18] Lopes DR, Silva CLP, Soares RB, Pereira PHR, Oliveira AC, Figueiredo RB, et al. Cytotoxicity and corrosion behavior of magnesium and magnesium alloys in Hank's solution after processing by high-pressure torsion. Adv Eng Mater 2019;21:1900391.
[19] Silva CLP, Oliveira AC, Costa CGF, Figueiredo RB, de Fátima Leite M, Pereira MM, et al. Effect of severe plastic deformation on the biocompatibility and corrosion rate of pure magnesium. J Mater Sci 2017;52:5992–6003.

[20] Medeiros MP, Lopes DR, Kawasaki M, Langdon TG, Figueiredo RB. An overview on the effect of severe plastic deformation on the performance of magnesium for biomedical applications. Materials 2023;16:2401.
[21] Bridgman PW. Effects of high shearing stress combined with high hydrostatic pressure. Phys Rev 1935;48:825–47.
[22] Roostaei M, Uggowitzer PJ, Pippan R, Renk O. Severe plastic deformation close to the melting point enables Mg-Fe nanocomposites with exceptional strength. Scr Mater 2023;230:115428.
[23] Castro MM, Montoro LA, Isaac A, Kawasaki M, Figueiredo RB. Mechanical mixing of Mg and Zn using high-pressure torsion. J Alloys Compd 2021;869:159302.
[24] Hernández-Escobar D, Unocic RR, Kawasaki M, Boehlert CJ. High-pressure torsion processing of Zn–3Mg alloy and its hybrid counterpart: a comparative study. J Alloys Compd 2020;831:154891.
[25] Hernández-Escobar D, Rahman ZU, Yilmazer H, Kawasaki M, Boehlert CJ. Microstructural evolution and intermetallic formation in Zn-Mg hybrids processed by High-pressure torsion. Philos Mag 2019;99:557–84.
[26] Carvalho AP, Assunção ACdO, Braga JdO, Lopes DR, dos Santos DMM, Nunes EHM, et al. Consolidation of Zn-Hydroxyapatite and Zn-Bioactive glass composites using high-pressure torsion. Crystals 2023;13:949.
[27] Lopes D, Soares RB, Castro MM, Figueiredo RB, Langdon TG, Lins VFC. Corrosion behavior in Hank's solution of a magnesium–hydroxyapatite composite processed by high-pressure torsion. Adv Eng Mater 2020;22:2000765.
[28] Castro MM, Lopes DR, Soares RB, dos Santos DMM, Nunes EHM, Lins VFC, et al. Magnesium-based bioactive composites processed at room temperature. Materials 2019;12:2609.
[29] Floriano R, Edalati K, Pereira KD, Luchessi AD. Titanium-protein nanocomposites as new biomaterials produced by high-pressure torsion. Sci Rep 2023;13:470.
[30] Sadighian S. Magnetic natural polymers' application as drug carriers. Biocomposite nanomaterials and their applications. Springer; 2024. p. 195–218.
[31] Zarei S, Sadighian S, Rostamizadeh K, Khalkhali M. Theragnostic magnetic core-shell nanoparticle as versatile nanoplatform for magnetic resonance imaging and drug delivery. Biointerface Res Appl Chem 2021;11:13276–89.
[32] Sadighian S. Metal and metal oxide–based nanostructures for drug delivery. Medical nanobiotechnology. Elsevier; 2025. p. 127–45.
[33] Zema L, Melocchi A, Maroni A, Gazzaniga A. Three-dimensional printing of medicinal products and the challenge of personalized therapy. J Pharmaceut Sci 2017;106:1697–705.
[34] Yang Y, Wu H, Fu Q, Xie X, Song Y, Xu M, et al. 3D-printed polycaprolactone-chitosan based drug delivery implants for personalized administration. Mater Des 2022;214:110394.
[35] Carvalho AP, Reis LM, Pinheiro RPRP, Pereira PHR, Langdon TG, Figueiredo RB. Using plane strain compression test to evaluate the mechanical behavior of magnesium processed by HPT. Metals 2022;12:125.
[36] Performance standards for antimicrobial disk susceptibility tests. Clinical and Laboratory Standards Institute; 2015. p. 96.
[37] Performance standards for antifungal susceptibility testing of yeasts. Clinical and Laboratory Standards Institute; 2017.
[38] Hernández-Escobar D, Kawasaki M, Boehlert CJ. Metal hybrids processed by high-pressure torsion: synthesis, microstructure, mechanical properties and developing trends. Int Mater Rev 2022;67:231–65.
[39] Castro MM, Sabbaghianrad S, Pereira PHR, Mazzer EM, Isaac A, Langdon TG, et al. A magnesium-aluminium composite produced by high-pressure torsion. J Alloys Compd 2019;804:421–6.
[40] Castro MM, Pereira PHR, Isaac A, Figueiredo RB, Langdon TG. Development of a magnesium-alumina composite through cold consolidation of machining chips by high-pressure torsion. J Alloys Compd 2019;780:422–7.
[41] Kormout KS, Pippan R, Bachmaier A. Deformation-induced supersaturation in immiscible material systems during high-pressure torsion. Adv Eng Mater 2017;19:1600675.
[42] Bachmaier A, Keckes J, Kormout KS, Pippan R. Supersaturation in Ag–Ni alloy by two-step high-pressure torsion processing. Philos Mag Lett 2014;94:9–17.
[43] Miyazaki T, Terada D, Miyajima Y, Suryanarayana C, Murao R, Yokoyama Y, et al. Synthesis of non-equilibrium phases in immiscible metals mechanically mixed by high pressure torsion. J Mater Sci 2011;46:4296–301.
[44] Silva C, Figueiredo RB, Gonzalez BM, Montoro LA, Isaac A. Designing ultrahard aluminum nanocomposites by severe mechanochemical processing. Mater Sci Eng A 2021;801:140422.
[45] Caires AJ, Castro MM, Montoro LA, Isaac A, Figueiredo RB. Redox reaction in a Mg/Nb2O5 nanocomposite processed by high-pressure torsion. Mater Lett 2021;303:130418.
[46] Wu Y-H, Bhatta L, Lee I, Figueiredo RB, Kawasaki M, Santala MK. Multi-scale characterization of supersaturated and intermetallic nanoscale phases in alloys produced by high-pressure torsion processing of Al and Mg sheets. JOM 2024.
[47] Edalati K. Metallurgical alchemy by ultra-severe plastic deformation via high-pressure torsion process. Mater Trans 2019;60:1221–9.